Fracture Mechanics of Concrete Structures
Proceedings FRAMCOS-3
AEDIFICATIO Publishers, D-79104 Freiburg, Germany

CONTRIBUTION TO THE ANALYSIS OF THE EFFECTS OF PORE PRESSURE ON THE THERMAL SPALLING OF CONCRETE AT HIGH TEMPERATURES

G. Heinfling and J.M. Reynouard
U.R.G.C.-Structures, INSA de Lyon, Villeurbanne, France
C. Duval
Division Mecanique des Structures, EDF-SEPTEN, Villeurbanne, France

Abstract

A computational method is proposed to account for the mechanical contribution of pore pressures in the analysis of the behaviour of concrete structures submitted to high temperatures. Considering concrete as an homogenous isotropic material, the temperature and pore pressure fields are derived from a coupled heat and moisture transport calculation. A thermo-plasticity based model is used for the analysis of the behaviour of the skeleton. The evolution of the hydraulics-mechanics coupling coefficient with temperature is experimentally identified. Experiments performed on high performance concrete specimens are simulated. The effect of pore pressure on the spalling failure mechanism is scrutinised.

Key words: Spalling; high temperatures

1 Introduction

In severe accidental situations such as fire or hypothetical core disruptive nuclear accident, reinforced concrete structures can be submitted to extremely high transient temperatures. High temperatures induce strong chemical and physical changes of the micro-structure of concrete that affect its mechanical behaviour. The major phenomena which have been identified include the release and evaporation of significant amount of water that induce pressure gradients under which water is transported towards the surface through pores. Experimental and theoretical analyses indicate that pore pressure built up could contribute to the explosive spalling of high performance concrete structures at elevated temperatures (Harmathy 1965, Meyer Ottens 1975, Zhukov 1976, Bazant et al. 1981, Noumowe et al. 1996, Anderberg 1997). These spalling phenomena are a major problem in the evaluation of the safety of concrete structures under such conditions.

The issue of the prediction of pore pressure under different conditions have been investigated by several authors (England and Skipper 1973, Bazant et al. 1981, Dayan and Gluekler 1982, Schneider and Herbst 1987, Kontani and Shah 1995, Jouhari and Lalaai 1997). In the seek of analysing spalling phenomena, most of the previously mentioned works have focused on the possible local mechanisms that could lead to spalling and are based on qualitative considerations. Very few studies deal with the numerical modelling of the mechanical effects of pore pressures on the behaviour of concrete structures at elevated temperatures. Within the framework of finite elements, a numerical method has been proposed by Majumdar et al (1995). However, in this study, the concrete was assumed to behave elastically and pore pressure was considered as a direct internal stress, regardless of the actual nature of concrete porous micro-structure.

Following the same general approach, we present here the first step of a numerical study which aims at providing a general numerical tool allowing for the non-linear analysis of the possible mechanical contribution of pore pressure in spalling phenomena. This paper focuses on an extension of a thermo-plasticity based model for concrete at elevated temperatures to account for pore pressures within the framework of the mechanics of porous media.

2 Constitutive equations

In the proposed approach, the concrete is considered as a porous medium which is a superposition of two interacting continuum media: the solid skeleton and a fluid phase inside the connected pores. This material is considered homogeneous and isotropic, and it is assumed that all the physical properties can be expressed as effective properties. An important assumption is that the transfer properties of concrete are considered to be only dependent on temperature, moisture and pore pressure. These are of course rather crude assumptions since damage can strongly affect the permeability and the porosity of concrete and can induce anisotropy of these properties (Gerard et al. 1996). The problem is then solved in two sequences. Temperature and pore pressures are first derived from a heat and moisture transfer analysis and are used as input for the stress analysis.

2.1 Heat and moisture transport calculations

Heat and moisture transports in concrete at elevated temperatures are highly coupled mechanisms. The mathematical model used in a previous study by Noumowe et al. (1996) for the coupled heat and moisture transport calculation of the tests presented further is based on the model of Bazant et al. (1981). The set of governing equations traducing coupled heat and moisture transport are given as follows. The conservation of mass is represented by:

$$\frac{\partial w}{\partial t} = -\operatorname{div} J + \frac{\partial w_d}{\partial t} \tag{1}$$

where t is the time, w is the free water content and w_d is the total mass of free water that has been released into the pores by dehydration of the cement matrix. The mass flux of moisture J is given by the Darcy's law:

$$J = -a \operatorname{grad} p \tag{2}$$

where a is the water permeability of concrete, and p is the pore water pressure. The conservation of energy is represented by:

$$\rho C \frac{\partial T}{\partial t} = C_a \frac{\partial w}{\partial t} + C_w J \operatorname{grad} T - \operatorname{div} q \tag{3}$$

where ρ is the unit mass of concrete, and C, C_a, C_w respectively are the isobaric heat capacities of concrete, adsorbed water and free capillary water. Finally, the heat transfer rate q is given by :

$$q = -k \operatorname{grad} T \tag{4}$$

where q is the heat flux and k is the heat conductivity of concrete. The material properties introduced are dependent on pore pressure and temperature. These governing equations are complemented by semi-empirical sorption isotherms, relating the free water content w, pressure p and temperature T. The finite element scheme is based on Galerkin method and a step by step solution with iterations is used for time integration of the nonlinear set of variational equations.

2.2 Definition of the effective stress

Within the framework of the mechanics of porous continua (Coussy 1995), and considering a thermo-poro-plastic behaviour for concrete, the effective stress vector σ' responsible for the deformation of the skeleton can be expressed in the following general form as a function of the total stress vector σ and pore pressure p:

$$\sigma' = \sigma + B_0\left[p + \varphi\left(\varepsilon, \varepsilon^P, p, T\right)\right] \tag{5}$$

where B_0 is the initial Biot's tensor. φ is a function describing its evolution with the deformation of the skeleton, pore pressure and temperature. ε and ε^P respectively are the total strain vector and the plastic strain vector of the skeleton. Considering the assumption of isotropy of the material and neglecting as a first approximation the effects of damage of the skeleton on the Biot's tensor, the effective stress can be expressed:

$$\sigma' = \sigma + b_0\left[1 + \varphi(p, T)\right]pi \tag{6}$$

where i is the identity vector and b_0 is the initial Biot's coefficient. For general porous materials, this coefficient is bounded below by the value of the porosity of the material Φ, and above by 1:

$$\Phi \leq b \leq 1 \tag{7}$$

For concrete, the Biot's coefficient can be assumed to be given by the porosity Φ which has been shown to be highly temperature dependent (Noumowe et al. 1996). The effective stress vector is then finally expressed by:

$$\sigma' = \sigma + \Phi_0\left[1 + \psi(p, T)\right]pi \tag{8}$$

where Φ_0 is the initial porosity of concrete and ψ is a function traducing its evolution with pore pressure and temperature.

Empirical laws implemented in TEMPOR 2 provides the evolution of porosity with pore pressure. The evolution of this parameter with temperature can be obtained from mercury porosimetry tests performed after cooling of concrete heated at different elevated temperatures (Noumowe et al. 1996).

2.3 Thermo-plasticity based model for the behaviour of the skeleton

The thermo-plastic behaviour identified for concrete (Heinfling et al. 1997) is supposed to hold true for the skeleton despite the fact that pore pressure can contribute to some of the experimental observations. The model proposed and implemented in the finite element code CASTEM2000 by these authors for concrete at elevated temperatures, is then used here for the analysis of the behaviour of the solid skeleton.

2.3.1 Incremental formulation

In this model, assuming small strains, the total strain rate of concrete $\dot{\varepsilon}$ is decomposed into the sum of an elastic strain rate $\dot{\varepsilon}^{e}$, a plastic strain rate $\dot{\varepsilon}^{p}$, a thermal expansion strain rate $\dot{\varepsilon}^{\theta}$ and a thermo-mechanical interaction strain rate $\dot{\varepsilon}^{tr}$:

$$\dot{\varepsilon}=\dot{\varepsilon}^{e}+\dot{\varepsilon}^{p}+\dot{\varepsilon}^{\theta}+\dot{\varepsilon}^{tr} \tag{9}$$

Elastic as well as inelastic properties are temperature dependent. Their variations with temperature are irreversible. The elastic strain rate determines the stress rate through the temperature dependent elastic stiffness ratio matrix D = D(T) which is assumed to be isotropic throughout this paper:

$$\dot{\sigma}=D\dot{\varepsilon}^{e}+\dot{D}\varepsilon^{e} \tag{10}$$

The temperature dependency of the mechanical properties correspond to a phenomenological description of the micro-structural and chemical changes that take place in heated concrete. In particular, drying shrinkage is implicitly taken into account through the variations of the coefficient of thermal expansion of concrete $\alpha = \alpha(T)$. The thermal strain rate is given by eq. (11), in which i is the identity vector:

$$\dot{\varepsilon}^{\theta}=\alpha\dot{T}i \tag{11}$$

Investigation tests on plain concrete have shown that the thermal deformation of concrete is strongly dependent on the stress applied during heating up (Anderberg and Thelandersson 1976). Thermo-mechanical interaction strains have then to be taken into account. The simple formula, proposed by Anderberg and Thelandersson (1976) in a one dimensionnal context, has been generalised to a multiaxial state of stress by de Borst and Peeters (1987) and has been successfully incorporated by Khennane and Baker (1992) in a thermo-plasticity model. According to these authors, the thermo-mechanical interaction strain rate can be written as :

$$\dot{\varepsilon}^{tr} = H\sigma'\dot{T} \tag{12}$$

where σ' is the effective stress vector , $\dot{T}$ is the rate of heating, and H, for an isotropic material is given :

$$H_{ijkl} = \frac{\alpha k}{f'_c}\left[-\gamma\delta_{ij}\delta_{kl} + \frac{1}{2}(1+\gamma)\left(\delta_{ik}\delta_{jl} + \delta_{il}\delta_{jk}\right)\right] \tag{13}$$

whith δ_{ij}, the Kronecker delta and $f'_c = f'_c(T)$, the temperature dependent uniaxial compression strength of concrete. k and γ are coefficients of thermo-mechanical interaction that can be evaluated from transient creep tests. For usual concrete, k varies from 1.8 and 2.35 and γ has been found to be equal to 0.285.

The temperature driven phenomenological descriptions of the strains and changes of physical properties, induced by the hygral modifications of the cement matrix, determine the limits of this kind of model. Heating rate sensitivity of the modifications of the mechanical properties have for example to be prescribed explicitely by the variation laws introduced in data. This is not straightforward for non-uniformly heated complex structures. However, simulations of tests performed on plain concrete specimens as well as reinforced concrete structures give satisfying results as soon as the parameters and their evolutions are identified under thermal and hygral conditions corresponding as closely as possible to the structure analysed (Heinfling et al. 1997).

As shown in Figure 1, a temperature dependent non smooth multi-surface criterion is used to describe the non symmetrical failure envelope of concrete. The Rankine criterion is used to bound the tensile strength:

$$\sigma_d \leq f'_t \tag{14}$$

where σ_d is the principal tensile stress in the principal direction d and $f'_t = f'_t(T)$ is the temperature dependent uniaxial tensile strength of concrete.

Biaxial compression tests performed at elevated temperatures show a significant increase in the sensitivity of compression strength to hydrostatic pressure with temperature (Ehm and Schneider 1985, Kordina et al. 1985). This makes the ultimate strength envelopes changing shape with temperature. In order to account for this effect, a Drucker-Prager type criterion changing shape with temperature is used to describe the failure surfaces of concrete under compression.

This criterion is given:

$$\sqrt{3J_2} + \eta I_1 - \mu f_c'(T) \le 0 \tag{15}$$

where I1 and J2 respectively are the first invariant of the stress tensor and the second invariant of the stress deviator and:

$$\eta = \frac{\beta - 1}{2\beta - 1} \quad \text{and} \quad \mu = \frac{\beta}{2\beta - 1} \tag{16}$$

where β = β(T) is the ratio of the biaxial compression strength to the uniaxial compression strength. The variations of β with temperature can be obtained from biaxial compression tests performed at different elevated temperatures. The experimental strength envelopes obtained by Kordina et al. (1985) are shown in figure 2 together with the model curves. The change of shape of the failure surfaces is captured and the agreement between the predicted and the experimental strength envelopes is acceptable.

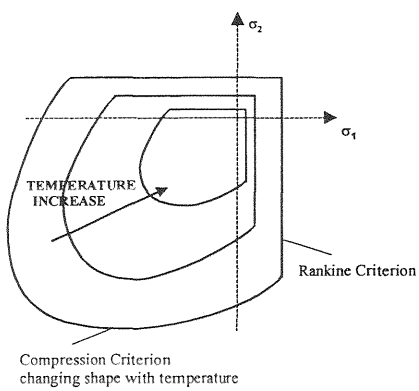

Figure 1: Failure criterion in two dimensional space with varying temperature

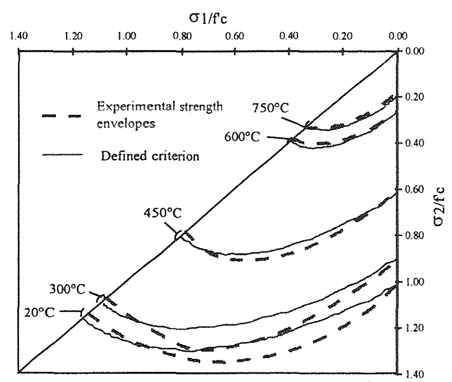

Figure 2: Experimental biaxial compression strength envelopes compared to the proposed criterion

Within the framework of multi-surface thermo-plasticity theory, the existence of yield surfaces f_i, function of stress σ, hardening parameter κ_i, and temperature T is assumed:

$$f_i(\sigma, \kappa_i, T) = 0 \tag{17}$$

Mode I cracking is described within this thermo-plasticity framework through tensile plastic flow. The isotropic Rankine flow theory proposed by Feenstra and de Borst (1995) is used. This approach corresponds to an isotropic smeared rotating description of cracking. The yield surfaces corresponding to the Rankine criterion are given:

$$f_1(\sigma', \kappa_1, T) = \sigma'_1 - \tau_1(\kappa_1, T) \tag{18}$$

where σ'_1 is the major principal tensile stress and $\tau_1(\kappa_1,T)$ is an equivalent stress which is given by a softening function of the internal parameter κ_1. This softening function is identified by the tensile strength f'_t and the temperature dependent tensile fracture energy $G_f = G_f(T)$ of concrete. The yield surfaces corresponding to the compression criterion are given:

$$f_2(\sigma', \kappa_2, T) = \frac{1}{\mu(T)}\left(\sqrt{3J_2} + \eta(T)I_1\right) - \tau_2(\kappa_2, T) \tag{19}$$

where $\tau_2(\kappa_2,T)$ is an equivalent stress which is given by a hardening/softening function of the internal parameter κ_2. This hardening/softening function is identified by the compressive strength f'_c and the temperature dependent compressive fracture energy $G_c = G_c(T)$ of concrete. The plasticity conditions are imposed on the two surfaces during the plastic flow:

$$\begin{cases} f_1(\sigma, \kappa_1, T) = 0 \\ f_2(\sigma, \kappa_2, T) = 0 \end{cases} \tag{20}$$

Isotropic hardening and associated plasticity are assumed for compression as well as tension plastic flow. The evolution of the plastic strain rate is given by the associated flow rule. The ambiguity of the plastic flow direction at the corner is removed according to Maier's proposal considering the contribution of each individual loading surface separately. In the general case where two loading surfaces are active, the plastic strain rate is then given:

$$\dot{\varepsilon}^p = \dot{\lambda}_1 \frac{\partial f_1}{\partial \sigma} + \dot{\lambda}_2 \frac{\partial f_2}{\partial \sigma} \tag{21}$$

where the $\dot{\lambda}_i$ are plastic multipliers that have to comply with the Kuhn-Tucker conditions:

$$\dot{\lambda}_i \geq 0, \quad f_i \leq 0, \quad \dot{\lambda}_i f_i = 0 \tag{22}$$

The Hillerborg method is employed in order to solve partially the pathological mesh dependency induced by the softening behaviour. An equivalent length related to the mesh size is then introduced in the definition of the $\tau(\kappa,T)$ laws.

It is assumed that the internal mechanical damage in the material as reflected in the internal parameter κ is governed by a work-hardening hypothesis. The internal variable is determined by the inelastic work rate $\dot{W}^p$ defined by:

$$\dot{W}^P = \sigma^T \dot{\varepsilon}^P = \tau(\kappa,T)\dot{\kappa} \tag{23}$$

Euler's theorem provides us the evolutionary equation for the two criteria:

$$\dot{\kappa}_i = \dot{\lambda}_i \tag{24}$$

2.3.b Thermo-plastic return mapping algorithm

A trapezoidal Euler backward scheme is used for the integration of the thermo-plastic constitutive equations. At the time step n+1, the updated effective stress vector σ'_{n+1} is obtained by:

$$\sigma'_{n+1} = \sigma'_e - D_{n+1}\left\{\Delta\lambda_1 \frac{\partial f_1}{\partial \sigma'} + \Delta\lambda_2 \frac{\partial f_2}{\partial \sigma'}\right\}_{n+1} \tag{25}$$

The thermo-elastic predictor σ'_e is obtained by freezing inelastic flow during the time step:

$$\sigma'_e = D_{n+1}\left(\Delta\varepsilon_{n+1} - \Delta\varepsilon^{th}{}_{n+1} - \Delta\varepsilon^{tr}{}_{n+1}\right) + \Delta D\varepsilon^e{}_n + \sigma'_n \tag{26}$$

Considering the evolutionary equation (22) and assuming uncoupling of tensile and compressive hardening, the problem finally consists of the determination of the inelastic incremental multipliers which enforce the plasticity conditions at the temperature T_{n+1}. In the general case where two loading functions are activate, this reads:

$$\begin{cases} f_1(\Delta\lambda_1, \Delta\lambda_2, T_{n+1}) = 0 \\ f_2(\Delta\lambda_1, \Delta\lambda_2, T_{n+1}) = 0 \end{cases} \tag{27}$$

A local Newton-Raphson method is used to solve this set of nonlinear equations. The updated inelastic incremental multiplier is calculated with help of a Broyden method.

2.3.c Equilibrium equations

The equilibrium equations resulting from the finite element discretisation are given:

$$K_{n+1}^{(i)} \Delta a_{n+1}^{(i+1)} = f_{ex\,n+1} + f_{p_{n+1}} - f_{in\,n+1}^{(i)} \tag{28}$$

where $K_{n+1}^{(i)}$ is the tangent stiffness matrix and $\Delta a_{n+1}^{(i+1)}$ is the nodal displacement vector increment and:

$$f_{p_{n+1}} = \int_V B^T b_{n+1} p_{n+1} i dV \tag{29}$$

is the pore pressure induced load vector, where B^T is the strain-nodal displacement matrix of the elements employed, b is the Biot's coefficient at T_{n+1} and i is the identity vector,

$$f_{in\,n+1}^{(i)} = \int_V B^T \sigma'^{(i)}_{n+1} dV \tag{30}$$

is the internal load vector and,

$$f_{ex\,n+1} = \int_V N^T F_{v_{n+1}} dV + \int_S N^T F_{s_{n+1}} dS \tag{31}$$

is the generalised external load vector where N^T is the interpolation matrix of the elements employed and F_V and F_S respectively are the body and traction forces vectors. The subscript n+1 refers to the time step and superscript (i) refers to the internal iteration during the solving process.

This set of non linear equilibrium equations is solved using the Newton-Raphson method.

3 Analysis of the behaviour of high strength concrete specimens

Tests performed by Noumowe et al. (1995) on high strength concrete specimens have been simulated. They have been carried out on axisymmetrical (16cmX32cm) specimens heated up at the controlled rate of 1°C/min.

Axisymmetrical calculations of pore pressures have been carried out by Noumowe et al. (1996) with help of TEMPOR2. The material parameters used in the computations are given in the corresponding paper. The boundary conditions applied uniformly on all the faces of the specimens were Dirichlet's type for temperature and perfect moisture transfer. Zero thermal and moisture fluxes were imposed on the symetry axis. The temperatures obtained were in agreement with the experimental measurements. The thermal gradient increased with the temperature rising, up to a maximum reached at about 325°C then decreased. It was very high near the heating surface (about 39°C/cm) and lower in the central part (about 2°C/cm). Figure 3 presents the temperature difference between the central part of the specimens and the surface as a function of the surface temperature. Figure 4 presents the distribution of the water vapour pressure on the radius of the specimens at middle heigth. The maximum pressure was found to increase with the temperature up to a maximum then decreased. It was observed that during heating, the pressure peak moved towards the centre of the specimen.

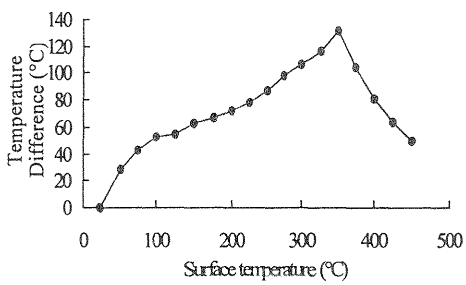

Figure 3: Temperature difference between the central part and the surface (Noumowe et al. 1996).

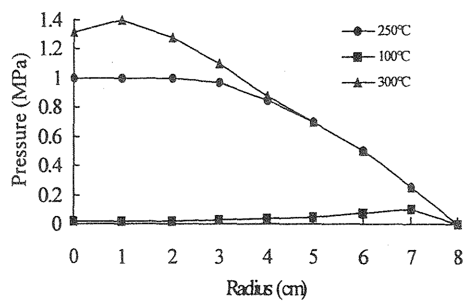

Figure 4: Distribution of pore pressure on the radius at middle heigth (Noumowe et al. 1996).

Figure 5 presents the evolution of the calculated pore pressure at the centre of the specimen as a function of the temperature at the surface. Results are compared with saturating vapour pressure values obtained from ASTM tables and with pressures obtained by Jouhari and Lalaai (1997) with a model formulated within the framework of the mechanics of open reactive porous media. It can be seen that the peak of pore pressure is predicted at the same temperature for the two coupled thermo-hygral analysis and that saturated vapour pressure is unable to provide a good estimation above this temperature.

Experimental observations indicate that about one third of the cylinders spalled explosively during heating. Spalling took place between 275°C and 350°C, in the rising phase of the thermal gradient. It is interesting to note that no spalling or explosion was observed when heating ordinary concrete specimens which presented almost the same experimental thermal gradients during heating up (Noumowe et al. 1996).

The temperature and pore pressure fields have been projected on the finite element mesh employed for the mechanical analysis presented in figure 7. The initial mechanical properties as well as their variations with temperature introduced in the computations are based on experimental measurements by Noumowe et al. (1996).

The results of the calculations a triaxial state of tensile stresses in the central part of the specimen, while, towards the surface, compressive stresses appear in the axial and cicumferential directions. Figure 7 presents the isovalues of the hardening parameter in tension obtained at different temperatures. Cracking occurs in the central part at 70°C, before significant pore pressure is build up in that part. The cracked zone is extending during heating up and reaches the top surface at 350°C. These results are consistent with the experimental observations of spalled specimens that describe a completely pulverised central zone (Noumowe et al. 1996). Figure 6 presents the hardening parameter in tension as a function of surface temperature. It can be observed that after 200°C on the surface, the hardening parameter that we can somehow relate to crack opening does not increase anymore. For the case where pore pressures are taken into account, this parameter increases up to a maximum value at 350°C which can be considered as the predicted failure temperature. Hence, we can consider that in these experiments, the spalling failure mode is initiated by thermal gradient only. However, it can be deduced from the compared crack propagation analysis that pore pressures can play a significant role in the kinetics of this failure mechanism since, as shown in figure 6, thermal loading only seem not to predict failure at 350°C.

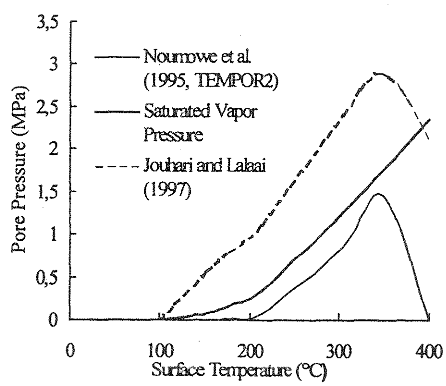

Figure 5: Calculated pore pressure in the central part of the specimens

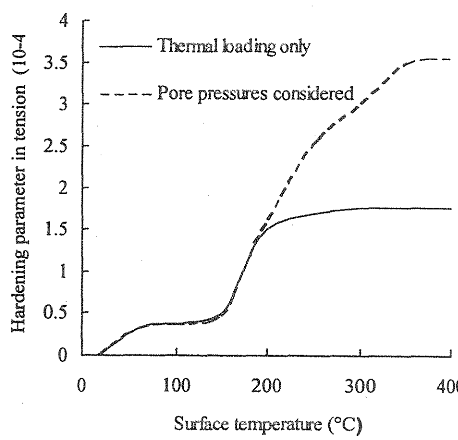

Figure 6: Hardening parameter in tension for a crack in the centre.

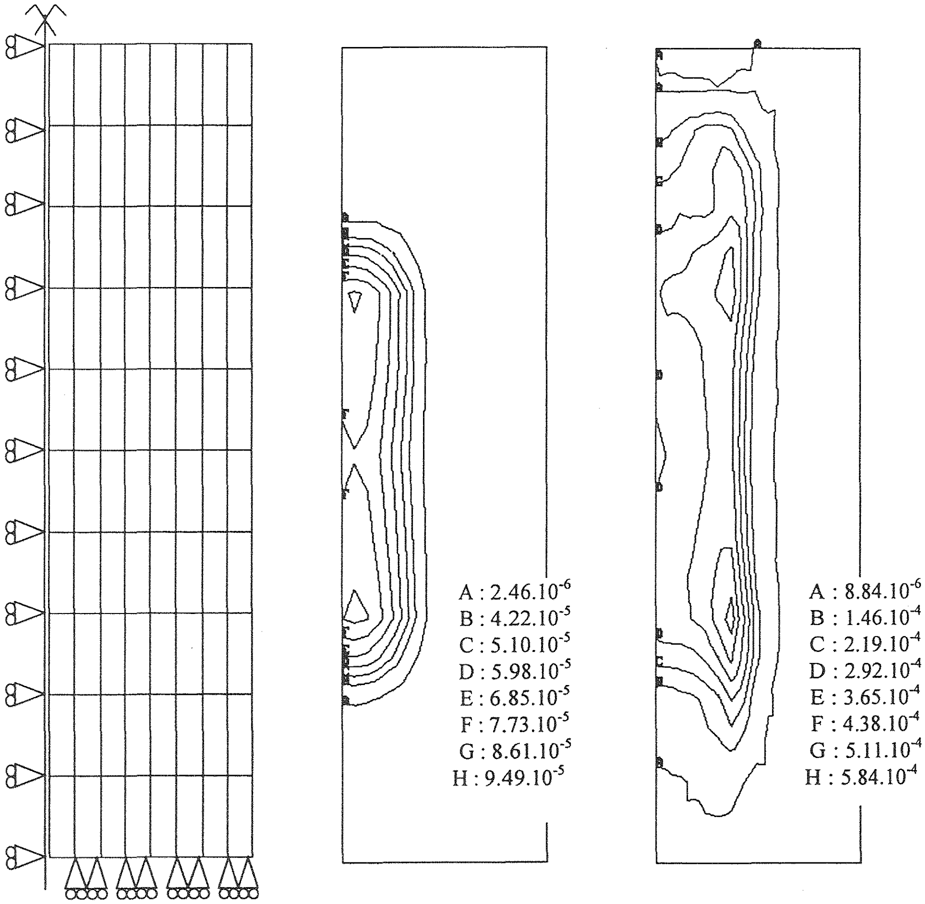

Finite element mesh　　　100°C on surface　　　350°C on surface

Figure 7: Tensile hardening parameter at different temperatures.

The results presented here are of course strongly influenced by the assumptions introduced for simplification of the problem. One has in particular to consider the effects of the local volume change induced by cracking on the evolution of pore pressure during heating. This volume increase could make pore pressure drop after cracking if diffusion cannot supply rapidly enough the mass of further steam to fill the dynamically expanding volume of the crack (Bazant 1997). One may also consider the possible increase of the Biot's tensor coefficients that would increase the effect of pore pressure on the effective stress. The issue of this possible cross effects should be scrutinized in the future.

4 Conclusions

Within the framework of the mechanics of porous continua, an extension of a thermo-plastic model to account for pore pressures has been proposed for the analysis of the behaviour of concrete at high temperatures.

This approach, based on simple assumptions is a first tool developed for the evaluation of the possible mechanical contribution of pore pressures to the spalling of concrete and to identify the main parameters involved in this contribution.

This model has been applied to the analysis of the behaviour of high strength concrete specimens submitted to high temperatures. Results emphasise that the predicted failure mechanism is in agreement with the experimental observations and that pore pressures can significantly affect the kinetics of this mechanism.

These results are of course influenced by the assumptions introduced for the simplification of the problem. Further developments are then needed in order to account for the effects of cracking on the heat and moisture transfer properties as well as on the hydraulics to mechanics coupling parameters such as the Biot's tensor.

These developments associated with an improvement of the thermo-plastic model allowing to account explicitly for dehydration effects would allow an accurate analysis of spalling mechanisms of concrete structures.

Finally, a closer examination of strain localization in the presence of coupled diffusive and mechanical phenomena involving softening behaviour should be undertaken in order to evaluate the objectivity of the numerical solution provided by this kind of analysis.

5 References

Anderberg, Y. (1997). Spalling phenomena of HPC. **In Proc. Int. Workshop on fire performance of high-strength concrete**, NIST, Gaithersburg, Maryland, 1997, NIST special publication, No. 919.

Anderberg, Y. & Thelandersson S. (1976). **Stress and deformation characteristics of concrete at high temperature.** Lund (Suede): Lund Institute of technology, 1976, 84p., Bulletin n°54.

Bazant, Z.P. (1997). Analysis of pore pressure, thermal stresses and fracture in rapidly heated concrete. **In Proc. Int. Workshop on fire performance of high-strength concrete**, NIST, Gaithersburg, Maryland, 1997, NIST special publication, No. 919.

Bazant, Z.P., Chern, J.C., Thonguthai, W. (1981). Finite element program for moisture and heat transfer in heated concrete. **Nuclear Engineering and Design**, 68, 61-70.

Coussy, O. (1995). **Mechanics of porous continua**. Chichester (U.K.): John Wiley & Sons.

Dayan, A. & Gluekler E.L. (1982). Heat and mass transfer within an intensly heated concrete slab. **Int. J; heat and mass transfer**, 25, 1461-1467.

de Borst, R. & Peeters, P.P.J.M. (1989). Analysis of concrete structures under thermal loading. **Comp. Meth. Appl. Mechs. Engng.**, 77, 293-310.

Ehm, C. & Schneider, U. (1985). The high temperature behavior of concrete under biaxial conditions. **Cement Concrete Res.**, 15, 27-34.

England, G.L. & Skipper M.E. (1973). On the prediction of moisture movement in heated concrete up to 550°C. **In Trans. 2nd SMIRT**, BAM, Berlin, 3, Paper H6/2.

Feenstra, P.H. & de Borst R. (1995). A plasticity model and algorithm for mode-I cracking in concrete. **Int. Journal Num. Meth. Engng**, 38, 2509-2529.

Gerard, B., Breysse D., Ammouche, A., Houdusse, O., Didry, O. (1996). Cracking and permeability of concrete under tension. **Materials and Structures**, 29, 141-151.

Harmathy, T.Z., (1965). Effect of moisture on the fire endurance of building materials. ASTM, Philadelphia, **ASTM Special Technical Publication** 385, 74-95.

Heinfling, G., Reynouard, J.M., Merabet, O., Duval, C. (1997). A thermo-elastic-plastic model for concrete at elevated temperatures including cracking and thermo-mechanical interaction strains. **In Proc. 5th COMPLAS**, Barcelona, 1493-1498.

Jouhari, L. & Lalaai, I. (1997). A constitutive model for thermo-hydro-chemo-mechanical response of decomposing high performance concrete under high temperature. **In Proc. 2nd Int. Conf. on Thermal Stresses and Related Topics**, Rochester, 221-224.

Kontani, O. & Shah S.P. (1995). Pore pressure in sealed concrete at sustained high temperatures. **Concrete Under Severe Conditions: Environment and loading** (Volume Two) Ed.by K. Sakai, N. Banthia and O.E. Gjorv, E & FN Spon, 1151-1162.

Khennane, A., Baker, G. (1992). Thermoplasticity model for concrete under transient temperature and biaxial stress. **In Proc. R. Soc. Lond.**, A, 439, 59-80.

Kordina, K., Ehm, C., Schneider, U. (1995). Effect of biaxial loading on the high temperature behavior of concrete. **In Proc. 1st Symp. of fire safety Science**, Gaithersburg, 281-290.

Majumdar, P., Gupta, A., Marchertas, A. (1995). Moisture propagation and resulting stress in heated concrete walls. **Nuclear Engineering and Design**, 156, 147-158.

Meyer-Ottens, C. (1975). Spalling of structural concrete under fire. **Deutscher Ausschuss für Stahlbeton**, Berlin (in German): W. Ernst & Sohn, Heft 248.

Noumowe, A., Clastres, P., Debicki, G., Costaz, J.L., (1996). Thermal stresses and water vapour pressure of high performance concrete at high temperature. **In Proc. 4th Int. Symp. on Utilisation of High-Strength/High-Performance concrete**, Paris, pp. 561-570.

Schneider, U. & Herbst H.J. (1987). Transport processes in thick concrete structures at high temperatures. **In Trans. 9th SMIRT**, 1987, H, 167-172.

Zhukov, V.V. (1976). Reasons of explosive spalling of concrete by fire. **Concrete and Reinforced Concrete**, 3.